AIP | Applied Physics Letters

Atomic scale investigations of ultra-thin GaInN/GaN quantum wells with high indium content

L. Hoffmann, H. Bremers, H. Jönen, U. Rossow, M. Schowalter, T. Mehrtens, A. Rosenauer, and A. Hangleiter

Citation: Applied Physics Letters **102**, 102110 (2013); doi: 10.1063/1.4795623
View online: http://dx.doi.org/10.1063/1.4795623
View Table of Contents: http://scitation.aip.org/content/aip/journal/apl/102/10?ver=pdfcov
Published by the AIP Publishing

Atomic scale investigations of ultra-thin GaInN/GaN quantum wells with high indium content

L. Hoffmann,[1,a)] H. Bremers,[1] H. Jönen,[1] U. Rossow,[1] M. Schowalter,[2] T. Mehrtens,[2] A. Rosenauer,[2] and A. Hangleiter[1]
[1]*Institute of Applied Physics, Technische Universität Braunschweig, Mendelssohnstrasse 2, 38106 Braunschweig, Germany*
[2]*Institute of Solid State Physics, Universität Bremen, 28359 Bremen, Germany*

(Received 1 February 2013; accepted 4 March 2013; published online 14 March 2013)

Using scanning transmission electron microscopy (STEM), we have studied ultra-thin (<2 nm) GaInN quantum wells (QWs) on c-plane GaN with high indium content (>25 %) suitable for blue-green light emitting devices. We are able to analyze the QW on an atomic scale with high resolution STEM and derive the indium content quantitatively. In our analysis, we find that indium is not only incorporated into the QW but also into the barriers under certain growth conditions. We observe indium tails or even plateau-like structures in the barriers, caused by excess indium being supplied during quantum well growth. © *2013 American Institute of Physics*. [http://dx.doi.org/10.1063/1.4795623]

While GaN-based blue light emitting devices exhibit exceptionally large external quantum efficiencies (EQEs > 84% (Ref. 1)), their green counterparts[2,3] quickly become less efficient at longer wavelengths, which is called the "green gap." To achieve higher emission wavelength, it is necessary to lower the band gap of the GaInN quantum well (QW) by increasing the indium content. However, such quantum wells are subject to a strong quantum-confined Stark effect due to piezoelectric fields[4] which leads to a spatial separation of electrons and holes and thus to a reduced radiative oscillator strength.[5] As the strain becomes larger at high indium content, this also holds for the piezoelectric fields leading to a much lower radiative transition probability and to a lower quantum efficiency.[6] To get rid of this problem, one solution is to decrease the QW thickness to less than 2 nm to increase the overlap of the electron and hole wave functions.[7] On the one hand, increasing the indium content increases the strain energy and decreases the critical thickness,[8] which leads to relaxation of the QW by defect formation.[9] Lattice faults are non-radiative centers, which reduce the quantum efficiency. On the other hand, with increasing indium content and decreasing QW thickness to several atomic rows, the influence of the QW thickness and the homogeneity within the QW on the oscillator strength and band gap increase drastically. For highly efficient QW structures, abrupt interfaces and a homogeneous indium distribution are needed. In this letter, we will discuss indium incorporation into ultra-thin QW structures on an atomic scale.

Our samples were grown by low pressure metal-organic vapor phase epitaxy on c-plane sapphire. The used precursors were trimethylgallium, triethylgallium, trimethylaluminum, trimethylindium, and ammonia. On sapphire, we used a nucleation layer to initiate growth followed by a 1.7 μm thick GaN buffer layer. The active region consisted of GaInN/GaN five-fold multi quantum well (MQW) structures with a QW thickness of about 1.5 nm and an indium content of 20% to 30%. In this work, all GaInN quantum wells have a growth temperature of 700 °C. For comparison, all samples are summarized in Table I.

The structural characterization was done by means of high resolution X-ray diffraction (HRXRD) and (scanning) transmission electron microscopy ((S)TEM). Using symmetrical, asymmetrical, and in-plane XRD scans, we were able to precisely deduce lattice constants, strain states, and finally the indium concentration in the QWs. For atomic scale investigations, we used a STEM technique developed by Rosenauer *et al.*[10] In this technique, electrons are detected, which are scattered to high angles (~35–300 mrad), using a high angle annular dark field (HAADF) detector. Recorded HAADF intensities (with specimen) are normalized to the intensity of the incoming electron beam by performing a scan of the electron beam over the HAADF detector without a sample. These normalized HAADF intensities can then be directly compared to image simulations and can be used to determine the specimen thickness in regions with known composition, e. g. GaN regions. The specimen thickness then is interpolated between the barrier layers. By comparison of the HAADF intensity in the QW region and the interpolated specimen thickness with simulations carried out as a function of specimen thickness and composition, concentrations within the QW region can be determined. Measured concentrations have been confirmed by atom probe tomography (APT) measurements. The samples are cross sections prepared using a focused ion beam (FIB); afterwards, the sample was ion-milled to remove amorphous

TABLE I. Overview of samples discussed in this work. The In/Ga flux ratio is given in mole fraction. The Ga flux ramping means an increase of gallium after the QW growth. The QW thicknesses derived from growth time, STEM, and XRD measurements are identical within the uncertainties.

Sample	In/Ga flux ratio	Ga flux	QW (nm)	T ramping
A	**2.7**	Const	1.5	Standard
B	**4.0**	Const	1.5	Standard
C1	4.0	**Ramping**	**1.0**	Standard
C2	4.0	Ramping	**1.9**	Standard
D	4.0	Const	1.5	**T+**

[a)]Electronic mail: lars.hoffmann@tu-braunschweig.de

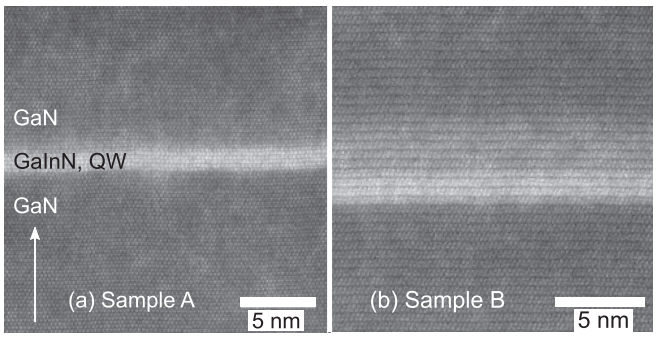

FIG. 1. Sample A and sample B. STEM images of the first QW of a 5-fold QW structure. Every dot correlates with an atomic row in electron beam and crystal direction [11$\bar{2}$0]. The growth direction is marked with a white arrow.

material from the surface. Just before the transfer into the STEM, the sample was plasma cleaned to avoid contamination within the STEM in interplay with the electron beam. The preparation technique is discussed in Ref. 11. The specimens were examined using a STEM FEI Titan with 300 keV acceleration voltage and a high angle annular dark field detector.

Fig. 1(a) shows a cross sectional STEM image of sample A focusing on the first QW in growth direction. The growth direction is marked with a white arrow. The preparation and beam direction are the [11$\bar{2}$0] zone axis (ZA). Every dot correlates with an atomic row in electron beam direction. The dark gray regions correspond to GaN, the GaInN QW is embedded in between. Due to the higher atomic mass of the indium in comparison to gallium, the GaInN QW has more intensity and will be depicted brighter.

To analyze the indium profile, we have integrated the indium content laterally along the QW and plotted it versus the relative length in growth direction in Fig. 2. The lower interface of the QW appears abrupt, the indium content turns out to be 24%, and the QW width is 1.5 nm. However, we have to mention that the upper QW interface is not as abrupt as the lower interface indicated by its slight tail.

In an attempt to increase the indium content, we have grown sample B with increased In/Ga ratio, which increases the available amount of indium in the system.

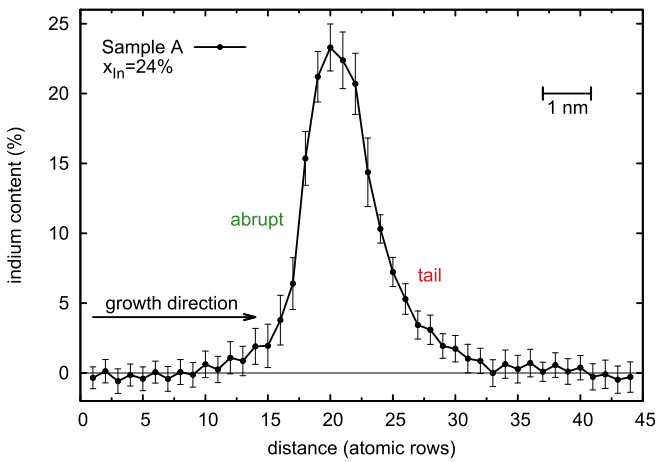

FIG. 2. Lateral integrated indium profile of the first QW of sample A from Fig. 1 plotted versus relative length in atomic rows along growth direction (arrow). The indium content has been derived from the intensity (Ref. 10); the error bars depict the standard deviation. The lower QW interface is abrupt, and the upper QW interface shows a tail.

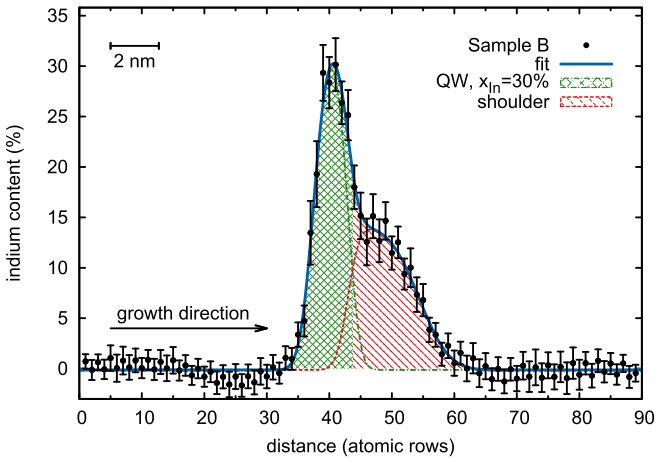

FIG. 3. Lateral integrated indium profile of the first QW (checkered) of sample B from Fig. 1 plotted versus relative length in atomic rows along growth direction (arrow). The fit is composed of a sum of error functions. The lower QW interface is abrupt, and the upper QW interface shows a shoulder (hatched).

Fig. 1(b) shows a STEM image of the first QW of sample B. The GaInN QW is clearly seen as the bright horizontal line embedded in the dark gray GaN. Above the QW, an additional lighter gray area appears. The line profile gives further details, which is shown in Fig. 3. The profile shows an abrupt lower QW interface and a maximum of about 30% of indium; but in this case, the upper interface becomes a kind of shoulder with an indium content of approximately 14%. This is unexpected since the indium source is closed during barrier growth. The indium incorporation in the barrier raises the question if the QW has been damaged and the indium originates from the QW itself during growth. In order to protect the QW with GaN layer, we introduce samples C1 and C2, where the gallium flux was increased directly after the QW to increase the growth rate and overgrow the QW as quickly as possible and to keep the indium in the QW. Samples C1 and C2 differ from each other only in the QW growth time. Figures 4(a) and 4(b) show STEM pictures of samples C1 and C2, respectively. The profile in Fig. 5 is for sample C2. Due to the beginning of relaxation in sample C2, which is confirmed by XRD (not shown) and the misalignment of the exact zone axis, the lateral resolution of the atom rows is weak. Once again, the lower interface of the QW is abrupt and the indium content is about 30%. The QW width

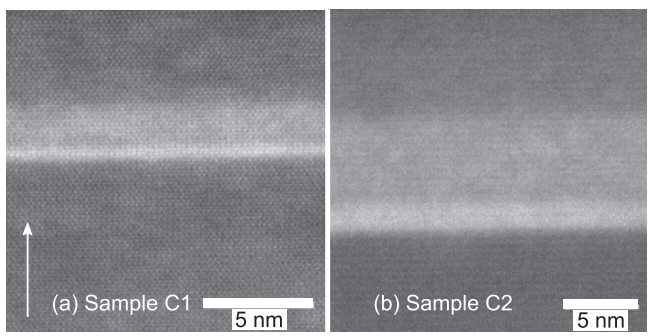

FIG. 4. Sample C1 and sample C2. STEM images of the first QW of a 5-fold QW structure, respectively. Every dot correlates with an atomic row in electron beam and crystal direction [11$\bar{2}$0]. The growth direction is marked with a white arrow.

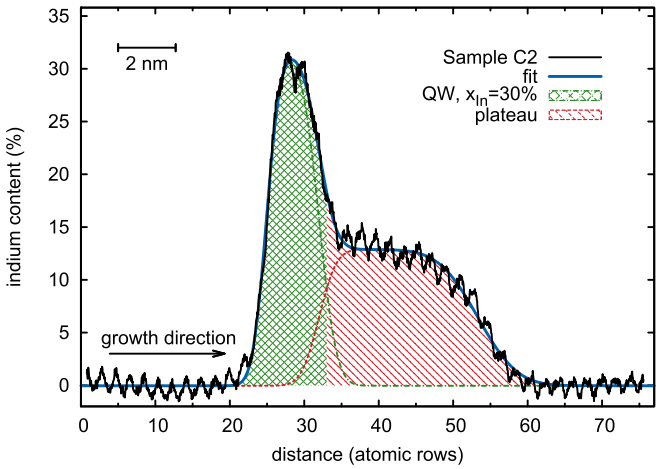

FIG. 5. Lateral integrated indium profile of the first QW (checkered) of sample C2 from Fig. 4 plotted versus relative length in atomic rows along growth direction (arrow). Due to the weak resolution of the image, we have to analyze the distance in growth direction in the one-dimensional case and must scale the distance to the given atomic rows. The lower QW interface is abrupt, and the upper QW interface shows a plateau (hatched).

correlates to the QW growth time. However, with the increased gallium flux, the upper QW interface becomes a plateau-like structure.

The large amount of indium in the barrier (about 14% indium, about 5 nm thickness) is comparable with the amount of indium in the quantum well (30% indium, 1.5 nm thickness). Adding up the indium content of the plateau-like structure of sample C2, we derive an equivalent of up to 3 monolayers of InN. In the literature, a wetting layer of up to two adlayers of indium during growth of GaInN is discussed.[12,13] Therefore, it is likely that this adlayer is incorporated into the barrier after the QW growth. Another option could be the build-up of nano-droplets of indium on the surface during growth, or finally there is the possibility that indium accumulates in open-core screw dislocations during QW growth, providing an indium source during barrier growth.

To minimize indium incorporation into the barrier, we introduce an extra temperature ramp T+ directly after quantum well growth, implemented in sample D. Due to the high vapor pressure of indium, the temperature ramping was introduced to lead to a desorption of the extra indium. However, great care is necessary to avoid damaging the QW.

A sketch of the temperature profiles versus growth time is given in Fig. 6. In previous work, we have discussed that pit formation can be suppressed and the homogeneity can be

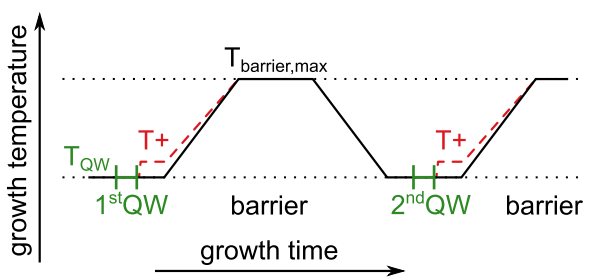

FIG. 6. Sketch of the temperature profile in the active zone. T+ describes the extra temperature ramp in the barrier just after QW growth to avoid indium incorporation into the barrier and differs from the standard temperature profile in the barrier.

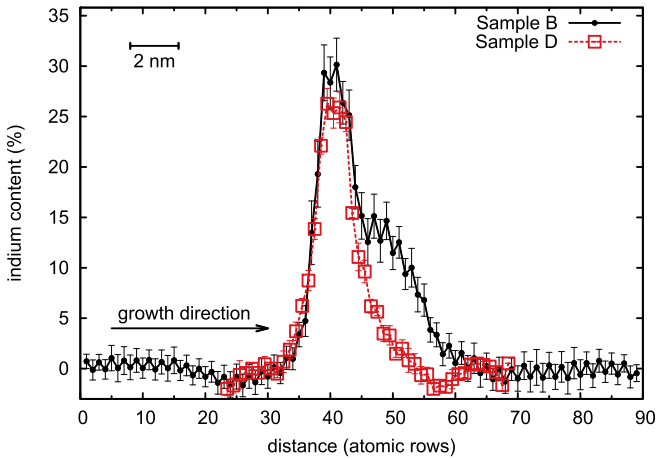

FIG. 7. Lateral integrated indium profile of the first QW of sample B from Fig. 3 and sample D (STEM not shown) plotted versus relative length in atomic rows along growth direction. Sample B is plotted with black fulfilled dots and sample D with red empty squares.

improved by ramping the growth temperature to $T_{barrier,max}$ in the barriers.[14] However, the temperature T_{QW} of 800 °C and lower is necessary to achieve a high indium content of 30% within GaInN QW. It turned out that covering the QW with GaN prior to ramping to $T_{barrier,max}$ is important.[14,15] The new results on atomic scale lead us to introduce this extra temperature ramp T+ = 740 °C. T+ must not be too low to evaporate the indium, but also not too high, to avoid damaging the QW. The standard ramp $T_{barrier,max}$ in the barrier is the same. Except for the T+ ramp, samples B and D are directly comparable and the profiles are shown in Fig. 7. The indium content and the shape are confirmed by XRD simulations (not shown). The comparison of the upper interface shows a reduction of the indium incorporation. The introduction of the new temperature profile leads to a reduction of the shoulder without reducing the indium content in the QW within the uncertainties.

In conclusion, we have demonstrated an atomic scale investigation of 1.5 nm ultra-thin GaInN/GaN QW's with an indium content of 30% using STEM and XRD. Depending on growth conditions, we observe an incorporation of indium into the barrier forming a plateau-like structure. The amount of indium is comparable with the amount of indium in the QW. For the origin of the indium in the plateau, several explanations are possible. The most likely reason is the incorporation of the indium adlayer during growth. To avoid the indium incorporation into the barrier, an extra temperature step direct after the QW growth is introduced to evaporate the indium adlayer. The indium content of the QW is not affected.

We gratefully acknowledge the financial support of the Bundesministerium für Bildung und Forschung (BMBF) in the frame of the "ERA-SPOT True Green (13N9634)" project. A. Rosenauer thanks the Deutsche Forschungsgemeinschaft for financial support under Contract RO 2057/8-1.

[1]Y. Narukawa, M. Ichikawa, D. Sanga, M. Sano, and T. Mukai, J. Phys. D: Appl. Phys. **43**, 354002 (2010).
[2]S. Nakamura, M. Senoh, N. Iwasa, and S. Nagahama, Jpn. J. Appl. Phys., Part 2 **34**, L797 (1995).

[3]S. Nakamura, M. Senoh, N. Iwasa, S. Nagahama, T. Yamada, and T. Mukai, Jpn. J. Appl. Phys., Part 2 **34**, L1332 (1995).
[4]T. Takeuchi, S. Sota, M. Katsuragawa, M. Komori, H. Takeuchi, H. Amano, and I. Akasaki, Jpn. J. Appl. Phys., Part 2 **36**, L382 (1997).
[5]J. Seo Im, H. Kollmer, J. Off, A. Sohmer, F. Scholz, and A. Hangleiter, Phys. Rev. B **57**, R9435 (1998).
[6]A. Hangleiter, J. Im, J. Off, and F. Scholz, Phys. Status Solidi B **216**, 427 (1999).
[7]D. Fuhrmann, C. Netzel, U. Rossow, A. Hangleiter, G. Ade, and P. Hinze, Appl. Phys. Lett. **88**, 071105 (2006).
[8]C. Kim, I. K. Robinson, J. Myoung, K. Shim, M.-C. Yoo, and K. Kim, Appl. Phys. Lett. **69**, 2358 (1996).
[9]A. D. Bykhovski, B. L. Gelmont, and M. S. Shur, J. Appl. Phys. **81**, 6332 (1997).
[10]A. Rosenauer, T. Mehrtens, K. Müller, K. Gries, M. Schowalter, P. V. Satyam, S. Bley, C. Tessarek, D. Hommel, K. Sebald, M. Seyfried, J. Gutowski, A. Avramescu, K. Engl, and S. Lutgen, Ultramicroscopy **111**, 1316 (2011).
[11]T. Mehrtens, S. Bley, P. V. Satyam, and A. Rosenauer, Micron **43**, 902 (2012).
[12]J. E. Northrup and C. G. V. de Walle, Appl. Phys. Lett. **84**, 4322 (2004).
[13]J. E. Northrup, Phys. Rev. B **79**, 041306 (2009).
[14]H. Jönen, U. Rossow, T. Langer, A. Dräger, L. Hoffmann, H. Bremers, A. Hangleiter, F. Bertram, S. Metzner, and J. Christen, J. Cryst. Growth **310**, 4987 (2008).
[15]D. Fuhrmann, H. Jönen, L. Hoffmann, H. Bremers, U. Rossow, and A. Hangleiter, Phys. Status Solidi C **5**, 1662 (2008).